Review of Scientific Instruments

RESEARCH ARTICLE | NOVEMBER 21 2024

Profiling a pulsed molecular beam with cavity-enhanced absorption spectroscopy

Zhuang Liu ; Qian-Hao Liu; Cun-Feng Cheng ; Shui-Ming Hu

Rev. Sci. Instrum. 95, 115108 (2024)
https://doi.org/10.1063/5.0227509

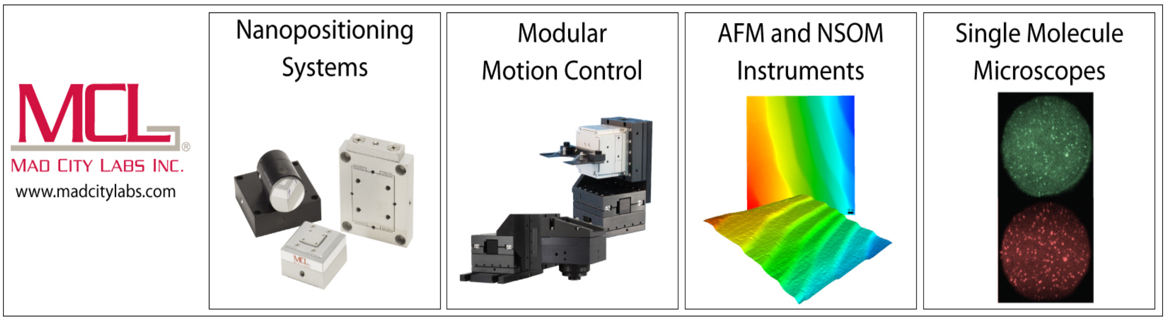

AIP Publishing

Review of
Scientific Instruments

ARTICLE

pubs.aip.org/aip/rsi

Profiling a pulsed molecular beam with cavity-enhanced absorption spectroscopy

Cite as: Rev. Sci. Instrum. 95, 115108 (2024); doi: 10.1063/5.0227509
Submitted: 9 July 2024 • Accepted: 2 November 2024 •
Published Online: 21 November 2024

Zhuang Liu, Qian-Hao Liu, Cun-Feng Cheng,[a)] and Shui-Ming Hu

AFFILIATIONS

State Key Laboratory of Molecular Reaction Dynamics, Department of Chemical Physics, University of Science and Technology of China, Hefei 230026, China

[a)]**Author to whom correspondence should be addressed:** cfcheng@ustc.edu.cn

ABSTRACT

The molecular beam plays an important role in chemical dynamics experiments. The density in the beam is one of the critical factors influencing the reaction rate in these studies. Here we present a method based on laser-locked cavity-enhanced absorption spectroscopy to measure the molecular density in the beam. The P(1) transition in the second overtone band of CO was measured in the molecular beam, demonstrating a determination of the number density of molecules in a specific quantum state from the absorption spectrum. This non-destructive spectroscopic method allows the measurement of state-resolved properties of a molecular beam, which could be applied to various studies such as molecular collision dynamics.

I. INTRODUCTION

Chemical reactions in the gas phase are essentially molecular scattering processes. Probing quantum states of chemical reactants and products is important for understanding the detailed structure of the interaction dynamics, which subsequently unveils the quantum nature of molecules. Advanced techniques, such as crossed molecular beam[1] and velocity map imaging,[2,3] make it possible to investigate molecular interactions at the quantum state-resolved level.[4–9] New advances have been made in the study of reactive resonances in several benchmark reactions using the state excitation method and quantum state-specific backward scattering spectroscopy. The relevant research provides an opportunity for a better understanding of molecular collisions.[10] However, detecting and characterizing these resonances pose considerable experimental challenges.

For instance, it is of great interest to observe resonances for polyatomic reactions[11–14] in scattering experiments or to investigate chemical reactions in the cold molecular system. Such experiments are likely to be very sensitive to the presence of reactive resonances since the quantum mechanical-related effects play important roles in the measurements of cross-sections and rate constants.[9,15,16] Current methods for measuring the molecular density in a beam rely mainly on ionization techniques, which in principle could detect single molecules.[17,18] However, the complex electronic structure limits ionization spectroscopy of most polyatomic molecules.[19] Careful calibration is required for ionization spectroscopy when absolute molecular densities are needed,[20] which adds complexity to the measurement of rate constants.

Infrared absorption spectroscopy, which relies on molecular vibrational structure rather than electronic structure, is a general method for molecular detection that provides high resolution and can be applied to most molecules. The cavity-enhanced absorption spectroscopy (CEAS) technique,[21] as a powerful analytical tool that utilizes high-finesse passive optical resonators to increase the effective optical path length, represents one of the most sensitive quantitative detection methods available. The developments of the laser-locked CEAS technique[22–24] allow the probe laser to be kept in resonance with the high-finesse cavity and monitoring the absorption continuously. Therefore, it would be possible to observe the reaction dynamics in a molecular beam.

In this work, we developed a scheme that uses the cavity-enhanced absorption technique to quantitatively measure the molecular density and the profile in a pulsed supersonic molecular beam. This approach allowed us to observe and analyze the behavior of molecules in a quantum state-resolved manner.

II. EXPERIMENT AND METHOD

The experimental setup is depicted in Fig. 1. A Parker General Valve (GV series 9, 0.1 mm orifice) was utilized to generate a molecular beam of CO operating with a pulse repetition rate of 5 Hz and an opening duration of 1.2 ms. The stagnation pressure was maintained at 6 bars while the background pressure in the vacuum chamber was ~10^{-2} Pa during valve operation.

We placed a high-finesse ($F = 100\,000$) cavity in the vacuum chamber downstream of the molecular beam. The cavity consists of a pair of high-reflectivity (HR, $R = 0.999\,97$) mirrors with a 2 m radius of curvature. The geometric distance between the two mirrors is about 65 cm, resulting in a free spectral range (FSR) of 230.6 MHz. The probe laser was a continuous-wave external cavity diode laser (ECDL) operating at 1575 nm with an output power of 30 mW. The laser was locked to the high-finesse optical cavity by the Pound–Drever–Hall (PDH) method,[25] and the laser frequency was kept in resonance with one cavity mode. The light transmitted from the cavity was monitored by a photodiode (Thorlabs, SM05PD5A) and recorded by an A/D converter with a sampling rate of 200 kSa/s.

A reference laser locked to an optical frequency comb (OFC) was used as the optical frequency reference. The OFC operated at 1–2 μm is synthesized by an Er:fiber oscillator with its repetition frequency (f_r) and carrier offset frequency (f_0) referenced to a rubidium clock disciplined to GPS, resulting in a fractional frequency accuracy at the level of 10^{-12}. The beat signal between the probe laser and the reference laser was fed to a phase-locked servo depicted in Fig. 1. A microwave function generator (MFG) was used as the microwave frequency reference. The feedback servo locked the beat signal at the microwave reference frequency by tuning a piezoelectric actuator (PZT) glued on one of the HR mirrors. Therefore, both the cavity length and the probe laser frequency are locked to the reference laser. Frequency scanning can be achieved by tuning the microwave reference frequency, and details of the locking and scanning schemes have been presented in our previous studies.[26,27]

A. Calibration of the absorption path length

Under the weak absorption approximation, the cavity-enhanced absorption can be described with Beer–Lambert's law, and the absorption path length is enhanced by a factor of $2F/\pi$ compared to its geometric length.[28] Monitoring the behavior of molecules in a selected quantum state, when they fly through the optical cavity, requires only detecting the transmission light, whereas obtaining the molecular number density needs to know the absorption path length. The ratio of the transmitted light intensity $I(\nu, T)$ to the incident light intensity $I_0(\nu)$ can be described as

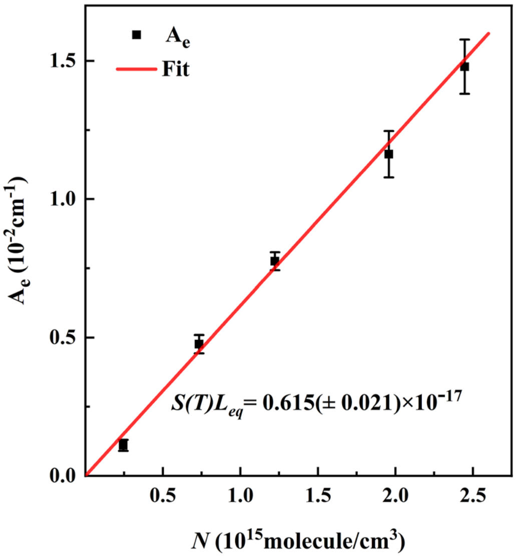

FIG. 2. Integrated absorbance of the P(1) line in the second overtone band at different number densities of CO measured by CEAS. The sample chamber was filled with pure carbon monoxide gas samples at 296 K.

$$I(\nu, T)/I_0(\nu) = \exp\{-S(T)N\varphi(\nu)L_{eq}\}, \tag{1}$$

where $S(T)$ is the spectral line intensity, which is available in the HITRAN database,[29] N is the number density of molecules, $\varphi(\nu)$ is the profile function, and L_{eq} is the equivalent absorption path length. Note that $S(T)$ is temperature dependent since the population of molecules at a given energy level varies with temperature, and the dependence can also be referenced to the HITRAN database. The integrated absorbance around the line at ν_0,

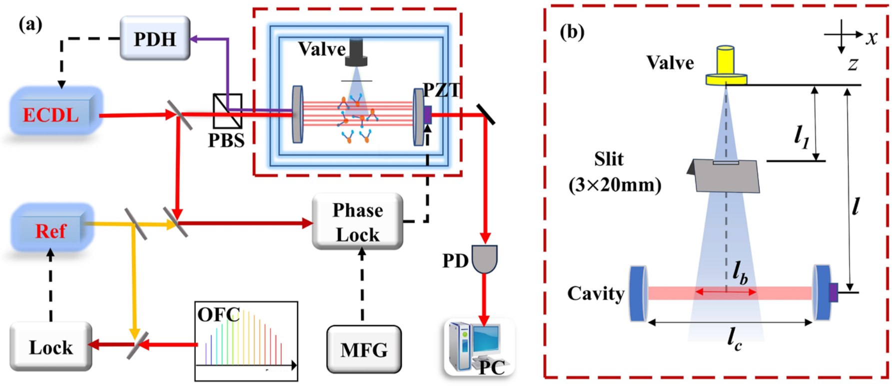

FIG. 1. (a) Configuration of the experimental setup. (b) Geometric schematics of the pulsed valve, slit, and optical cavity in the chamber (l_1 = 15 mm, l = 50 mm, l_b: length of beam, l_c = 646 mm:length of cavity). ECDL, external cavity diode laser; Ref, reference laser; MFG, microwave function generator; OFC, optical frequency comb; PBS, polarization beam splitter; PZT, piezoelectric actuator; PC, computer; PD, photodiode.

$$A_e = \int_{\nu_0-\Delta\nu}^{\nu_0+\Delta\nu} d\nu \ln \frac{I_0(\nu)}{I(\nu, T)} = S(T)NL_{eq}, \quad (2)$$

can be used to retrieve the molecular number density if $S(T)$ and L_{eq} are known.

It is essential to calibrate the absorption path length in quantitative CEAS measurements.[30,31] We determine the effective path length of the cavity in its geometric length, l_c, by measuring the absorption spectrum of thermally equilibrated molecules before we get the overlap length, l_b, between the molecular and the laser beams. Figure 2 shows the measured integrated absorbance under different pressures of the static pure CO sample gas filled in the whole vacuum chamber at the room temperature of 296 K. Note that the horizontal axis has been converted to the molecular number density using the ideal gas equation, and the slope of the linear fit in Fig. 2 is $6.15 \pm 0.21 \times 10^{-16}$ cm^2/molecule. Taking the spectral line intensity of the P(1) line in the second overtone band of CO at 296 K given in the HITRAN database, we obtained an equivalent absorption length of 14.99 ± 0.49 km for the cavity.

B. Molecular density measurement

The key to measuring the density of a molecular beam is to obtain the effective absorption length of the beam. Here we estimate the effective absorption length of the beam according to the geometric relationship of molecular beam velocity, divergence angle, and slit geometry. The thermodynamic picture of adiabatic jet expansion can well describe the supersonic jet expansion of a fluid system into a vacuum. In the limiting case of small beam temperature $T_1 \ll T_0$, the maximum terminal flow velocity in a supersonic jet expansion of an ideal gas can be expressed as[32]

$$<v_{max}> = \sqrt{\frac{2R\gamma(T_0)}{m(\gamma-1)N_A}}, \quad (3)$$

where the gas constant $R = 8.314\,472$ J/(mol K), the heat capacity ratio γ is 7/5 for an ideal diatomic gas, and $T_0 = 296$ K. Therefore, the maximum terminal velocity of 784 m/s was estimated for a supersonic beam of CO. Taking into account the experimental conditions and combining our previous experiments with the molecular time-of-flight method, the longitudinal velocity value of 780 m/s is used in this work as a demonstration for molecular density determination. Thus, the geometric length l_b shown in Fig. 1 could be calculated if the transverse speed is known, which was obtained from the Doppler broadening of the absorption spectrum, and then the L_{eq} value under the beam condition could also be determined.

In a supersonic jet expansion, the equivalent temperature of the molecules in the beam is generally related to factors associated with experimental conditions, such as molecular species, background pressure, nozzle shape, and slit structure. The rotational temperature of the molecular beam depends on the population of rotational energy levels, which can usually be fitted experimentally by measuring the relative strengths of two or more rotational transitions. In this work, we simply assume the equivalent rotational temperature of about 5 K as an approximation to get the line intensity $k(T)$ value of the P(1) $(v = 3 - 0)$ line, and we can determine the molecular number density according to Eq. (2).

III. RESULTS AND DISCUSSION

The laser frequency was locked at the transition center of the P(1) line in the second overtone band of $^{12}C^{16}O$ and the light transmitted from the high-finesse cavity was measured. As depicted in Fig. 3, a time-resolved signal was observed when the pulsed valve was turned on. The signal looks similar to the time-of-flight (TOF) signal employed in ion detection schemes. When the molecular beam passes through the laser beam in the cavity, the transmittance signal decreases due to the molecular absorption. It is worth noting that the arrival of the molecular pulse significantly changes the refractive index between the two mirrors of the high-finesse cavity, which can break the lock of the laser. The signal can only be observed when the PDH locking servo has sufficient bandwidth and a large enough capture range to follow the change in the refractive index. We compared the signals when the plunger spring of the pulsed valve is adjusted tightly (shown in Fig. 3 in black) or loosely (shown in Fig. 3 in red). Although both signals have a primary peak of comparable amplitude, the latter one shows an additional minor peak with a 2 ms delay time after the primary peak, indicating gas leakage induced by poppet bounce, in agreement with the discussion presented in Ref. 33. The absorption signal is directly proportional to the molecular density, which allows us to characterize the molecular distribution in the supersonic jet without ionizing the molecules. This leads to non-destructive and *in situ* measurements.

The laser transmittance of the high-finesse cavity was recorded as the laser frequency was locked at various frequencies near the resonance. A similar time-dependent signal was obtained at each frequency. For each delay time, different locking points indicate the spectroscopic detuning with respect to the center frequency of the transition. Thus, the absorbance can be presented in terms of absorption spectra as shown in Fig. 4(a). The spectra can be well-fitted with a Gaussian function that corresponds to the transverse velocity distribution of moving molecules. The resulting Gaussian linewidth varies from 351 to 437 MHz. The additional broadening, such as the transit-time broadening of <1 MHz, the natural linewidth of <100 Hz, the laser linewidth of 2.3 kHz, and other possible

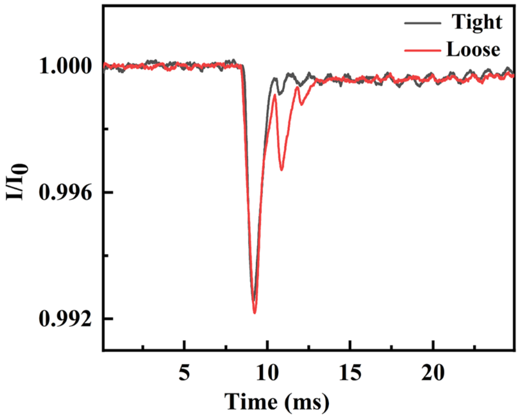

FIG. 3. Observed transmittance of the high-finesse cavity when the pulsed valve is turned on. The zero point on the time axis indicates the trigger applied to the valve. The black and red curves are the measured signal when the plunger spring of the valve is adjusted to be "tight" and "loose," respectively.

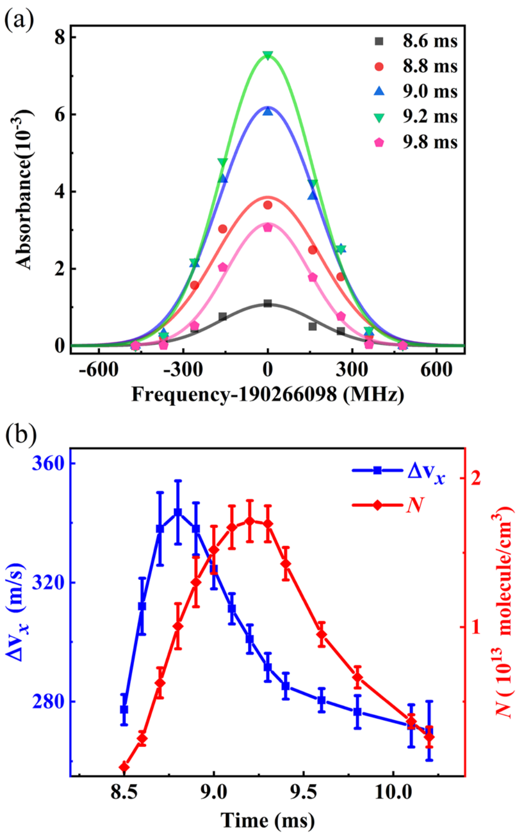

FIG. 4. (a) Linewidth of Gaussian fitting of the jet at different times. (b) Comparing transverse velocity distribution and molecular beam density at different times.

broadening factors, are negligible in our analysis. The homogeneous broadening beyond the velocity spread provides insight into the molecular interaction, enabling the investigation of molecular energy transfer in the inelastic collisions.[34] From those spectra, the transition frequency can be determined to be 190 266 097.8 MHz with a statistical uncertainty of 0.5 MHz. A discrepancy of −4.4 MHz is observed when compared with the result of saturated absorption spectroscopy with comb-locked cavity ring-down spectrometer.[35] The residual first-order Doppler shift that comes from the non-perpendicular alignment between the central velocity of the molecular beam and the laser beam may be the main source of the shift.

In this work, we used the Gaussian width of the spectrum, corresponding to the transverse velocity distribution of molecules in the beam, to estimate the equivalent absorption length and determined the molecular density from the integrated area of the absorption peak. As shown in Fig. 4(b), the transverse velocity and the molecular density vary over time, as depicted with the blue and red lines, respectively. There is a delay of about 0.5 ms between the peaks of the blue and red curves. This delay is likely caused by the presence of hot molecules in the beam, which have greater velocity spread and arrive at the probe region earlier than the colder molecules with a smaller velocity spread. The transverse speed ranges from 280 to 340 m/s, the calculated l_b value is 35.5–44.1 mm, and the corresponding L_{eq} value is 0.82–1.02 km. The molecular density for each time delay is then determined according to the absorbance and L_{eq}. It is noteworthy that the distribution of molecular density along the beam direction exceeds the duration of the valve opening, and there is a substantial position spread in the beam. Since the cooling effect of the molecular beam relies on parameters such as the nozzle opening and stagnation pressure, our method offers a direct way to measure the molecular velocity and density distributions, and such information could be very useful in chemical dynamics studies.

Based on the above experimental results, the molecular density can be expressed in the time-velocity domain, resulting in a three-dimensional profile of a pulsed molecular beam, as shown in Fig. 5. In particular, the profile gives the beam velocity distribution of the beam over time for a single quantum state, which could help to detect reactants and products in the molecular collisions in the gas phase. In our experiment, the high-finesse cavity is linear, which refers to the information along the x-direction only in Fig. 1. The orthogonal cavity along the y-direction, perpendicular to the molecular beam, can also be used to obtain the complete transverse information.

The experiment provides a universal cavity-enhanced absorption detection technique applicable to infrared-active molecules. This method is particularly advantageous for detecting molecules that cannot be identified by the REMPI method, such as certain complex polyatomic molecules. By employing a continuous wave laser and the cavity locking technique, the resolution of the laser source has achieved a precision of up to kilohertz. In Fig. 4(a), transverse velocity spread, or spectral width, emerges as the main limitation of the measured spectral resolution, which is currently sufficient for resolving the rotational transitions. Further reduction of the molecular beam divergence would significantly enhance the high-resolution detection capabilities for larger molecules.

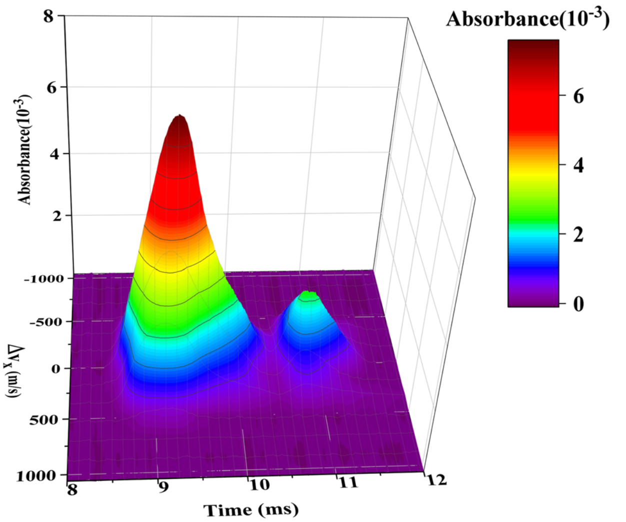

FIG. 5. Absorption spectrum of the P(1) line (6346.59 cm^{-1}) in the second overtone band of CO.

IV. CONCLUSION

The scheme based on the laser-locked cavity-enhanced absorption technique is used to measure the absolute number density in a molecular beam. As a demonstration, we conducted measurements of the P(1) transition in the second overtone band of CO. The results show that the setup is capable of observing the molecular beam in both the frequency and time domains. We assume that the maximum number density of the measured beams is $1.7 \pm 0.1 \times 10^{13}$ molecule/cm^3, with a detection limit of about 2×10^{11} molecule/cm^3 over 1000 shots. The experimental method could be applied to most molecules with infrared transitions, such as C_2H_2, H_2O, CH_4, and so on. If a stronger line in the fundamental band of the interested molecule is used, the detection limit could be improved by three orders of magnitude, providing a sensitive detection scheme for polyatomic molecules. The non-destructive technique enables the detection of molecules and measurement of molecular properties before or after collisions. Such a valuable detection tool paves the way for assessing chemical reaction products and reactants and determining the rate constants of chemical reactions.

ACKNOWLEDGMENTS

This work was jointly supported by the National Natural Science Foundation of China (Grant Nos. 22241302, 22327801, and 11974328) and the Chinese Academy of Science (Grant No.YSBR-055).

AUTHOR DECLARATIONS

Conflict of Interest

The authors have no conflicts to disclose.

Author Contributions

Zhuang Liu: Data curation (equal); Formal analysis (equal); Visualization (equal); Writing – original draft (equal); Writing – review & editing (equal). **Qian-Hao Liu**: Data curation (equal); Formal analysis (equal); Investigation (equal). **Cun-Feng Cheng**: Funding acquisition (equal); Investigation (equal); Methodology (lead); Project administration (lead); Resources (equal); Writing – original draft (equal); Writing – review & editing (equal). **Shui-Ming Hu**: Supervision (equal); Writing – original draft (equal); Writing – review & editing (equal).

DATA AVAILABILITY

The data that support the findings of this study are available from the corresponding author upon reasonable request.

REFERENCES

[1] Y. T. Lee, "Molecular beam studies of elementary chemical processes," Science **236**, 793–798 (1987).

[2] A. T. J. B. Eppink and D. H. Parker, "Velocity map imaging of ions and electrons using electrostatic lenses: Application in photoelectron and photofragment ion imaging of molecular oxygen," Rev. Sci. Instrum. **68**, 3477–3484 (1997).

[3] D. W. Chandler and P. L. Houston, "Two-dimensional imaging of state-selected photodissociation products detected by multiphoton ionization," J. Chem. Phys. **87**, 1445–1447 (1987).

[4] T. Wang, J. Chen, T.-G. Yang, C.-L. Xiao, Z.-G. Sun, L. Huang, D.-X. Dai, X.-M. Yang, and D.-H. Zhang, "Dynamical resonances accessible only by reagent vibrational excitation in the F + HD → HF + D reaction," Science **342**, 1499–1502 (2013).

[5] T.-G. Yang, J. Chen, L. Huang, T. Wang, C.-L. Xiao, Z.-G. Sun, D.-X. Dai, X.-M. Yang, and D.-H. Zhang, "Extremely short-lived reaction resonances in Cl + HD ($v = 1$) → DCl + H due to chemical bond softening," Science **347**, 60–63 (2015).

[6] D.-F. Yuan, Y.-F. Guan, W.-T. Chen, H.-L. Zhao, S.-R. Yu, C. Luo, Y.-X. Tan, T. Xie, X.-A. Wang, Z.-G. Sun, D.-H. Zhang, and X.-M. Yang, "Observation of the geometric phase effect in the H + HD → H_2 + D reaction," Science **362**, 1289–1293 (2018).

[7] Y.-R. Xie, H.-L. Zhao, Y.-F. Wang, Y. Huang, T. Wang, X. Xu, C.-L. Xiao, Z.-G. Sun, D.-H. Zhang, and X.-M. Yang, "Quantum interference in H + HD → H_2 + D between direct abstraction and roaming insertion pathways," Science **368**, 767–771 (2020).

[8] W.-T. Chen, R.-S. Wang, D.-F. Yuan, H.-L. Zhao, C. Luo, Y.-X. Tan, S.-H. Li, D.-H. Zhang, X.-A. Wang, Z.-G. Sun, and X.-M. Yang, "Quantum interference between spin-orbit split partial waves in the F + HD → HF + D reaction," Science **371**, 936–940 (2021).

[9] J. J. Lin, J.-G. Zhou, W.-C. Shiu, and K. Liu, "State-specific correlation of coincident product pairs in the F + CD_4 reaction," Science **300**, 966–969 (2003).

[10] T. Wang, T.-G. Yang, C.-L. Xiao, Z.-G. Sun, D.-H. Zhang, X.-M. Yang, M. L. Weichman, and D. M. Neumark, "Dynamical resonances in chemical reactions," Chem. Soc. Rev. **47**, 6744–6763 (2018).

[11] W.-C. Shiu, J. J. Lin, and K. Liu, "Reactive resonance in a polyatomic reaction," Phys. Rev. Lett. **92**, 103201 (2004).

[12] H.-L. Pan, K. Liu, A. Caracciolo, and P. Casavecchia, "Crossed beam polyatomic reaction dynamics: Recent advances and new insights," Chem. Soc. Rev. **46**, 7517–7547 (2017).

[13] M. C. Babin, M. DeWitt, J. A. Lau, M. L. Weichman, J. B. Kim, H.-W. Song, H. Guo, and D. M. Neumark, "Observation of resonances in the transition state region of the F + NH_3 reaction using anion photoelectron spectroscopy," Nat. Chem. **15**, 194–199 (2023).

[14] S. Liu, J. Chen, X.-R. Zhang, and D.-H. Zhang, "Feshbach resonances in the F + CHD_3 → HF + CD_3 reaction," Chem. Sci. **14**, 7973–7979 (2023).

[15] M. Tizniti, S. D. Le Picard, F. Lique, C. Berteloite, A. Canosa, M. H. Alexander, and I. R. Sims, "The rate of the F + H_2 reaction at very low temperatures," Nat. Chem. **6**, 141–145 (2014).

[16] G.-Q. Tang, M. Besemer, S. Kuijpers, G. C. Groenenboom, A. van der Avoird, T. Karman, and S. Y. T. van de Meerakker, "Quantum state-resolved molecular dipolar collisions over four decades of energy," Science **379**, 1031–1036 (2023).

[17] J. J. Lin, J.-G. Zhou, W.-C. Shiu, and K. Liu, "Application of time-sliced ion velocity imaging to crossed molecular beam experiments," Rev. Sci. Instrum. **74**, 2495–2500 (2003).

[18] X.-M. Yang, "Probing state-to-state reaction dynamics using H-atom Rydberg tagging time-of-flight spectroscopy," Phys. Chem. Chem. Phys. **13**, 8112–8121 (2011).

[19] H.-W. Li and A. G. Suits, "Universal crossed beam imaging studies of polyatomic reaction dynamics," Phys. Chem. Chem. Phys. **22**, 11126–11138 (2020).

[20] Y. T. Hsu, J.-H. Wang, and K. Liu, "Reaction dynamics of O(^{1}D) + H_2, D_2, and HD: Direct evidence for the elusive abstraction pathway and the estimation of its branching," J. Chem. Phys. **107**, 2351–2356 (1997).

[21] M. Mazurenka, A. Orr-Ewing, R. Peverall, and G. A. D. Ritchie, "4 Cavity ring-down and cavity enhanced spectroscopy using diode lasers," Annu. Rep. Sect. C: Phys. Chem. **101**, 100–142 (2005).

[22] L. Gianfrani, S.-M. Hu, and W. Ubachs, "Advances in cavity-enhanced methods for high precision molecular spectroscopy and test of fundamental physics," Riv.Nuovo Cimento **47**, 229 (2024).

[23] G. Berden, R. Peeters, and G. Meijer, "Cavity-enhanced absorption spectroscopy of the 1.5 μm band system of jet-cooled ammonia," Chem. Phys. Lett. **307**, 131–138 (1999).

[24] J. Wang, Y. R. Sun, L.-G. Tao, A.-W. Liu, T.-P. Hua, F. Meng, and S.-M. Hu, "Comb-locked cavity ring-down saturation spectroscopy," Rev. Sci. Instrum. **88**, 043108 (2017).

[25] R. W. P. Drever, J. L. Hall, F. V. Kowalski, J. Hough, G. M. Ford, A. J. Munley, and H. Ward, "Laser phase and frequency stabilization using an optical resonator," Appl. Phys. B **31**, 97–105 (1983).

[26] J. Wang, Y. R. Sun, L.-G. Tao, A.-W. Liu, and S.-M. Hu, "Communication: Molecular near-infrared transitions determined with sub-kHz accuracy," J. Chem. Phys. **147**, 091103 (2017).

[27] Q.-H. Liu, Y.-N. Lv, C.-L. Zou, C.-F. Cheng, and S.-M. Hu, "Saturated absorption spectroscopy of HD at 76 K," Phys. Rev. A **106**, 062805 (2022).

[28] L. Gianfrani, R. W. Fox, and L. Hollberg, "Cavity-enhanced absorption spectroscopy of molecular oxygen," J. Opt. Soc. Am. B **16**, 2247–2254 (1999).

[29] I. E. Gordon, L. S. Rothman, R. J. Hargreaves, R. Hashemi, E. V. Karlovets, F. M. Skinner, E. K. Conway, C. Hill, R. V. Kochanov, Y. Tan, P. Wcisło, A. A. Finenko, K. Nelson, P. F. Bernath, M. Birk, V. Boudon, A. Campargue, K. V. Chance, A. Coustenis, B. J. Drouin, J. M. Flaud, R. R. Gamache, J. T. Hodges, D. Jacquemart, E. J. Mlawer, A. V. Nikitin, V. I. Perevalov, M. Rotger, J. Tennyson, G. C. Toon, H. Tran, V. G. Tyuterev, E. M. Adkins, A. Baker, A. Barbe, E. Canè, A. G. Császár, A. Dudaryonok, O. Egorov, A. J. Fleisher, H. Fleurbaey, A. Foltynowicz, T. Furtenbacher, J. J. Harrison, J. M. Hartmann, V. M. Horneman, X. Huang, T. Karman, J. Karns, S. Kassi, I. Kleiner, V. Kofman, F. Kwabia-Tchana, N. N. Lavrentieva, T. J. Lee, D. A. Long, A. A. Lukashevskaya, O. M. Lyulin, V. Y. Makhnev, W. Matt, S. T. Massie, M. Melosso, S. N. Mikhailenko, D. Mondelain, H. S. P. Müller, O. V. Naumenko, A. Perrin, O. L. Polyansky, E. Raddaoui, P. L. Raston, Z. D. Reed, M. Rey, C. Richard, R. Tóbiás, I. Sadiek, D. W. Schwenke, E. Starikova, K. Sung, F. Tamassia, S. A. Tashkun, J. Vander Auwera, I. A. Vasilenko, A. A. Vigasin, G. L. Villanueva, B. Vispoel, G. Wagner, A. Yachmenev, and S. N. Yurchenko, "The HITRAN2020 molecular spectroscopic database," J. Quant. Spectrosc. Radiat. Transfer **277**, 107949 (2022).

[30] B. J. Orr and Y. He, "Cavity-based absorption spectroscopy techniques," in *Laser Spectroscopy for Sensing*, edited by M. Baudelet (Woodhead Publishing, 2014), pp. 167–207.

[31] C. M. Rushworth, J. Davies, J. Cabral, P. Dolan, J. Smith, and C. Vallance, "Cavity-enhanced optical methods for online microfluidic analysis," Chem. Phys. Lett. **554**, 1–14 (2012).

[32] W. Christen, K. Rademann, and U. Even, "Supersonic beams at high particle densities: Model description beyond the ideal gas approximation," J. Phys. Chem. A **114**(42), 11189–11201 (2010).

[33] A. R. Barnea, E. Narevicius, J. Narevicius, M. Vinetsky, and U. Even, "Improved design for a highly efficient pulsed-valve supersonic source with extended operating frequency range," Rev. Sci. Instrum. **92**, 015110 (2021).

[34] W. E. Perreault, N. Mukherjee, and R. N. Zare, "Quantum control of molecular collisions at 1 kelvin," Science **358**, 356–359 (2017).

[35] J. Wang, C.-L. Hu, A.-W. Liu, Y. R. Sun, Y. Tan, and S.-M. Hu, "Saturated absorption spectroscopy near 1.57 μm and revised rotational line list of $^{12}\mathrm{C}^{16}\mathrm{O}$," J. Quant. Spectrosc. Radiat. Transfer **270**, 107717 (2021).